SPEED DIAGRAM OF A FAST FOILING SAILBOAT

M. Rabaud, Université Paris-Saclay, CNRS, FAST, 91405, Orsay, France, marc.rabaud@universite-paris-saclay.fr.

Foiling multihulls are now capable of sailing much faster than the wind in all directions, so they are in fact sailing always close to the apparent wind. We will discuss some general consequences of these high speeds and in particular: (i) the existence of a hysteresis cycle with two very different speeds for the same wind and heading conditions, (ii) transformations in the speed diagram which gives the boat speed in all sailing directions, (iii) the possibility of having not to ease but to trim in the sails during a bear-away and (iv) the effect of the atmospheric boundary layer on the twist angle of the sails of fast boats.

NOMENCLATURE

Symbol	Definition	(unit)
C_D	Drag coefficient	
C_{Di}	Induced drag coefficient	
C_L	Lift coefficient	
F_a	Aerodynamical forces	(N)
F_h	Hydrodynamical forces	(N)
L_f	Span of the foils	(m)
b_f	Chord of the foils	(m)
M	Mass of the boat	(kg)
G	Vertical wind gradient	(m^{-1})
S_f	Horizontal foil surface	(m^2)
$\mathbf{V}_a$	Apparent wind speed (AWS)	(m/s)
$\mathbf{V}_b$	Boat speed	(m/s)
$\mathbf{V}_t$	True wind speed (TWS)	(m/s)
$\mathbf{V}_c$	Take-off velocity	(m/s)
X	Speed ratio V_b/V_t	
z_0	Altitude of reference	(m)
β	Apparent wind angle (AWA)	(°)
γ	True wind angle (TWA)	(°)
ρ_w	Density of water	$(kg.m^{-3})$

1   INTRODUCTION

Over the last few decades, architects and shipbuilders have succeeded in greatly reducing the hydrodynamic drag of sailing yachts, first by reducing their weight, then by modifying hull shapes to facilitate planing and, today, by adding foils that allow the hull to be partially or totally lifted out of the water. As a result, sailing speeds have been greatly increased, and now exceeding 40 knots for long periods of time is relatively common for the new foiling multihulls or the AC75 monohulls of the next America cup. All the actions that allow such a foiling transition are therefore very important to win races. Furthermore, as the boat speeds become significantly greater than the true wind speed (TWS), the decrease of the apparent wind angle (AWA) and the concomitant increase of the apparent wind speed (AWS) have important consequences on the speed diagram of these fast boats. The objective of this paper is to present the transformations induced by these high speeds, using simple physical and analytical arguments. We will discuss successively the take-off speed, the possible existence of a hysteresis in the speed diagram, and some consequences of the modifications of the speed diagram induced by these flight conditions.

2   TRANSITION WITH HYSTERESIS TO FULL-FOILING SAILING

Hydrofoils are submerged surfaces used to generate lift and in particular vertical lift to partially or totally replace the hydrostatic lift. Above a critical boat speed V_c, the hull can be entirely lifted above sea level when only the appendages remain in contact with the water.
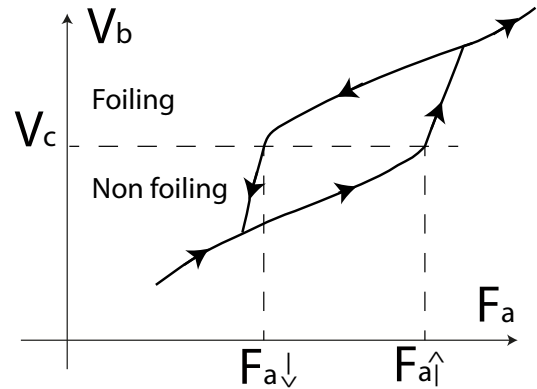

Figure 1: Sketch of the boat speed hysteresis curve occurring for increasing and decreasing aerodynamic forces F_a. The boat is foiling when $V_b > V_c$. The foiling transition occurs for increasing wind speed when the aerodynamic propulsive force reaches $F_{a\uparrow}$ while for decreasing wind speed the loss of this flight condition occurs for a lower aerodynamic force $F_{a\downarrow}$.

When sailing in a constant direction, if the wind velocity increases, the aerodynamic propulsive force F_a will also in-

crease and eventually become larger than a critical value $F_{a\uparrow}$ for which the boat velocity becomes larger than the foiling velocity V_c (figure 1). As the boat starts to fly, the hydrodynamic drag strongly decreases and thus its velocity increases significantly. It is thus possible to reduce the incidence angle of the foils, the so called "rake angle", while keeping constant the lift force. If the foil incidence is reduced, the hydrodynamic drag decreases further more and the boat will continue to accelerate. Now if the wind decreases, starting from a high value, as the hydrodynamic drag is smaller in foiling condition than in non-foiling one, the boat will remain above the sea surface until a smaller value of the aerodynamic force $F_{a\downarrow}$. Thus in the range $F_{a\downarrow} < F_a < F_{a\uparrow}$ the boat speed will have two different values depending of the past conditions. In this range, the existence of a hysteresis cycle will have enormous consequence in the strategy to win a race. All maneuvers as pumping, surfing or transitory changes of direction that could trigger such foiling transition must be sought.

2.1 CRITICAL FOILING VELOCITY

In order to be fully foiling, the boat speed V_b must exceed a take-off velocity V_c corresponding to the fact that the vertical lift generated by the foils becomes larger than the boat weight. This condition writes $\frac{1}{2}\rho_w V_c^2 S_f C_L = Mg$, where ρ_w is the water density, S_f the total horizontal surface of the foils, C_L the lift coefficient of the foils and M the total mass of the boat. Thus the critical take-off velocity is:

$$V_c = \sqrt{\frac{2Mg}{\rho_w S_f C_L}}, \tag{1}$$

For example for the sailing trimaran Gitana 17, the take-off velocity is $V_c \approx 22$ knots for a total horizontal foil surface $S_f = 4\,m^2$ and a total mass $M = 15\,500$ kg. Using these data and Eq. 1 we obtain that the mean lift coefficient of the foils should be $C_L \approx 0.6$. This value seems reasonable as it corresponds for example to a rake angle (incidence angle of the foils) of $5°$ if one assume a classical NACA0012 profile [1], or no more than a few degrees for a more sophisticated cambered foil section. Furthermore, assuming this NACA profile and this rake angle, the corresponding 2D drag coefficient is $C_D \approx 0.015$. We must also add the induced drag due to the finite aspect ratio of the foils [12, 4, 13]. The induced drag coefficient can be estimated as $C_{Di} = \frac{b_f}{\pi L_f} C_L^2$ where L_f is the individual foil span and b_f its chord. This induced drag corresponds to the force needed to generate the vorticity present at the tip or the elbow of the foil. For example with $L_f = 1.5$ m, $b_f = 0.5$ m one finds $C_{Di} \approx 0.038$. Thus the induced drag is larger than twice the 2D drag, and the lift-to-drag ratio is of the order of 10. Finally, adding also the drag on the vertical part of the foils and on the immersed part of the rudders one could estimate the total hydrodynamic drag at take-off velocity to be of the order of 15 000 N, a tenth of the weight of the boat.

2.2 SPEED DIAGRAMS IN FOILING OR NON FOILING CONDITIONS

The speed diagram is a polar plot that represents, for a given TWS and a given sea state, the speed of the boat V_b in all sailing directions γ [8]. These velocities are target velocities and assume the best possible tuning of sails and foils.

In the range of wind speeds where the boat may or may not be foiling depending on past conditions, it is interesting to plot the two corresponding speed diagrams in order to look for a trajectory in the plane (V_b, γ) that crosses the circle $V_b = V_c$ and allows to pass from the low velocity curve (non-foiling) to the high velocity curve (foiling). Indeed, assuming that for a given heading γ_1 the boat navigates at velocity $V_1(\gamma_1) < V_c$ it may be possible to bear-away or to come up to another angle γ_2 in order to overtake V_c and start foiling and then return to the initial course angle γ_1 but now on the hight velocity curve $V_2(\gamma_1) > V_c$. A similar behavior was recently found by a 6DOF simulation of an ocean-racing trimaran [10], showing that a substantial speed difference could be obtained after a bear-away as a function of the transient trimming of the sails.

3 SPEED DIAGRAM OF FAST FOILING BOAT

The term fast ship here means fast in relation to wind speed. It is then useful to introduce a speed ratio $X = V_b/V_t$, ratio between the speed of the boat and TWS. Values of X between 2 and 3 are now common for some fully-foiling sailboats. We will now describe some consequences of sailing at $X > 1$.

3.1 DECREASE IN APPARENT WIND ANGLE

The apparent wind is the wind measured on board. It corresponds to the vectorial composition of the true wind $\mathbf{V}_t$ and the boat speed $\mathbf{V}_b$, represented on the figure 2. Note that traditionally, in the sailing world, γ and β are the angles between $\mathbf{V}_b$ and $-\mathbf{V}_t$ or $-\mathbf{V}_a$.

This vectorial equation $\mathbf{V}_a = \mathbf{V}_t - \mathbf{V}_b$ corresponds to two scalar relations:

$$V_a \cos\beta = V_t \cos\gamma + V_b \tag{2}$$
$$V_a \sin\beta = V_t \sin\gamma \tag{3}$$

or introducing the speed ratio:

$$\tan\beta = \frac{\sin\gamma}{\cos\gamma + X} \tag{4}$$
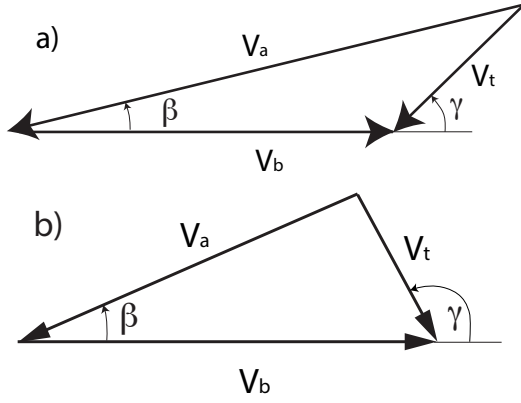$$V_a = V_t\sqrt{1 + 2X\cos\gamma + X^2}. \tag{5}$$

Figure 2: Velocities composition between the true wind speed $\mathbf{V}_t$ and the boat speed $\mathbf{V}_b$ which gives the apparent wind speed $\mathbf{V}_a$: (a) upwind ($\gamma < 90°$) on port tack for $X = 2.2$, (b) downwind ($\gamma > 90°$) on port tack for $X = 2.2$.

It is clear from these equations that for small X, the distinction in strength and direction between true and apparent wind is weak, but for large X the effect becomes significant, and β decreases with X for all γ angles. As a result, fast sailing boats navigate always at small AWA and with sheet-in sails. This is why it is not easy from photos to say whether these boats are sailing upwind or downwind.

Figure 3 shows the evolution of AWA for all possible sailing directions relative to the wind, assuming a constant speed ratio. AWA is maximum when TWA is $\gamma = \pi/2 + \beta$ and its value is then $\beta_{max} = \arcsin(1/X)$. For example, sailing at $X = 3$ means a maximum AWA of $20°$. The large values of X are therefore limited by the fact that sailboats, even when using rigid sails with large aspect ratio (and thus large lift-to-drag ratios), can not progress rapidly when AWA becomes too small.

3.2 SPEED DIAGRAM OF A BOAT SAILING AT A CONSTANT APPARENT WIND ANGLE

As hydrofoil yachts sail fast and therefore with a high speed ratio, there velocities are limited by their ability to sail efficiently with a small AWA. If we assume that this condition is indeed the dominant limitation, they will sail in all possible directions with that small constant value of $\beta = \beta_0$. We may wonder what the shape of the speed diagram would be for such a boat? This question first arose for ice-boats because, since the ice friction is very low, they can navigate at a value of X greater than 4 [11].

Figure 4 shows that, to navigate at a constant apparent wind angle β_0, the point M, at the origin of the vector $\mathbf{V}_b$, must see the segment AB (vector $\mathbf{V}_t$) at a constant angle. Point M thus
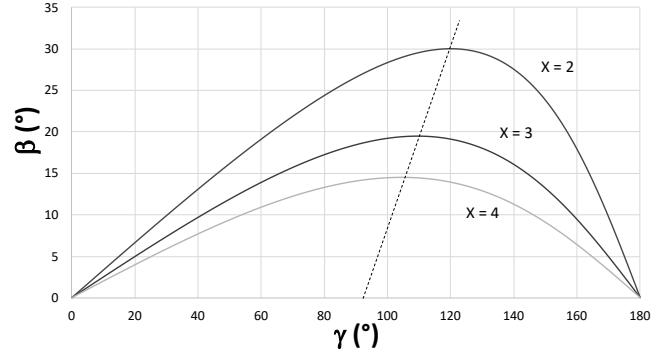

Figure 3: Evolution of the apparent wind angle β with respect to the true wind angle γ for constant speed ratio $X = 2, 3$ and 4 (Eq. 4). The dashed line corresponds to the place of β_{max}, maximum of the curve $\beta(\gamma)$, for all X: $\gamma(\beta_{max}) = \frac{\pi}{2} + \arcsin(1/X)$.

describes the arc of a circle ACB. Point A would correspond to a sailboat going in the wind direction at the wind speed ($X = 1$), point B to a sailboat stopping facing the wind ($X = 0$). Point C corresponds to the maximum speed for the boat $X_{max} = 1/\sin\beta_0$. The boat speed (and X) increases from A to C, then decreases to zero from C to B. The arc of circle ACB will be larger for a constant wind (AB fixed) the smaller the angle β_0 is, indeed the circle radius is $R = V_t/(2\sin\beta_0)$, which confirms that, to go fast with a given true wind, one must be able to sail with a low AWA.
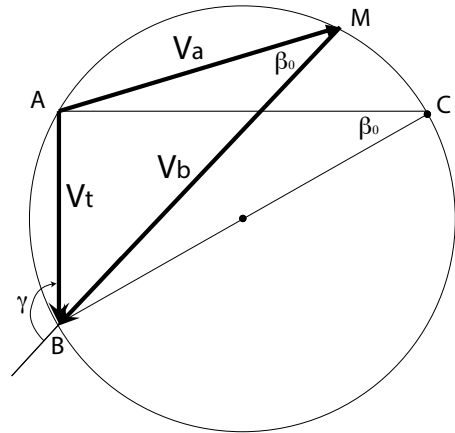

Figure 4: Diagram showing the geometrical condition for sailing on a starboard tack at $\beta_0 = 30°$. Point M can take any position between A and B on the arc of circle (ACB). Adapted from Ref. [3].

The speed diagram $V_{b0}(\gamma)$ corresponding to the condition of sailing at constant β_0 is drawn on the figure 5. It is deduced from the figure 4 by symmetry of point M with respect to B. It

is thus also a circular arc of the same radius R, or more exactly 2 circular arcs due to the left/right symmetry with respect to BA' for the port tack.
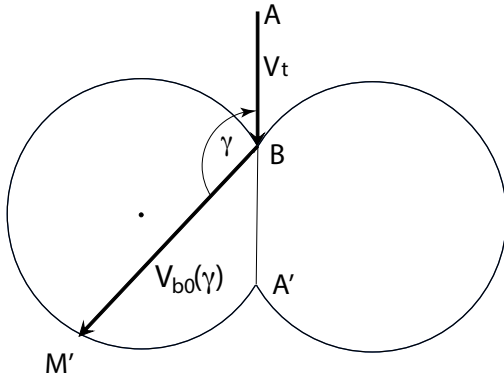

Figure 5: Speed diagram $V_{b0}(\gamma)$ under both tacks for a boat sailing at constant AWA $\beta_0 = 30°$. Points A' and M' are symmetrical of A and M (see figure 4) with respect to point B.

The speed diagram equation can be obtained from Eq. 4:

$$V_{b0}(\gamma) = V_t \left(\frac{\sin \gamma}{\tan \beta_0} - \cos \gamma \right) \qquad (6)$$

for γ in the $[\gamma_1, \gamma_2]$ range. The angle γ_1 corresponds to point B and is the smallest solution of Eq. 4 for $X = 0$ and $\beta = \beta_0$ while the angle γ_2 corresponds to point A' and is the largest solution of Eq. 4 for $X = 1$ and $\beta = \beta_0$. The second arc of circle on the right of figure 5 corresponds to the port tack and is obtained by left/right symmetry of the starboard arc BM'A'. Note that for an hypothetic boat sailing at constant speed ratio X_0 the speed diagram would also be a circle but centered on point B in figure 5.

3.3 NECESSARY CONDITION FOR HAVING TO TRIM THE SAILS DURING A BEAR-AWAY

On classical sailboats, during a bear-away (increase of γ) the apparent wind angle β also increases and the crew eases the sheets to optimize the angle of incidence of the sails. On a faster boat, the increase in boat speed during the maneuver induces a smaller increase of AWA. The limiting case, where it is no more necessary to ease the sheets during the maneuver corresponds to a constant β angle, as described in § 3.2. The polar plot is then, at least in the range of angle corresponding to the maneuver, an off-center circle as in figure 5.

A question now arises: is it possible to have to trim-in the sails when bearing away? That will be the case if β decreases as γ increases, so if $d\beta/d\gamma < 0$. Assume that we know the speed diagram of the boat $V_b(\gamma)$ for a given wind force V_t, the

derivation of Eq. 4 with respect to γ gives the condition:

$$\frac{dX}{d\gamma} > \frac{1 + \cos \gamma X}{\sin \gamma}. \qquad (7)$$

As $X = V_b/V_t$ this equation also writes:

$$\frac{dV_b}{d\gamma} > \frac{V_t + V_b \cos \gamma}{\sin \gamma}. \qquad (8)$$

This condition will be fulfilled if the local slope of the polar curve is greater than the slope for the same γ of the 2-circles polar curve of figure 5, i.e. if the real speed curve $V_b(\gamma)$ of the boat crosses at this angle γ, from inside to outside, the curve $V_{b0}(\gamma)$ given by the equation 6.

Table 1 gives the minimum value of the relative increase in boat speed required after a $10°$ bearing to have to trim the sheets in.

	$X = 1$	$X = 2$	$X = 3$
$\gamma = 50°$	37%	26%	22%
$\gamma = 90°$	17%	9%	6%
$\gamma = 120°$	10%	–	–

Table 1: Relative increase in boat speed $\Delta V_b/V_b$ after a $10°$ bearing required to have a decrease and not an increase of β for three initial TWA γ and three different speed ratios X.

4 TWIST OF THE SAILS OF A FAST SAILBOAT

Until now a constant true wind force was considered. However, due of the existence of the atmospheric boundary layer, the wind intensity increases with altitude z [7]. This evolution of V_T with z has an effect on the value of the AWA β which also becomes a function of z and thus on the optimal twisting of the sails [5, 6]. I will analyse now the consequence of sailing at high X on the optimal twist of the sails.

In the atmospheric boundary layer, the wind is stronger at higher altitudes and decreases, in theory to zero, at the sea surface. Since the airflow is turbulent, the velocity profile is generally described as logarithmic on a typical thickness that is highly dependent on the weather conditions (e.g. thermal stratification, humidity, convection, etc) and typical thicknesses of 200 to 500 m are often observed [9].

One can write this logarithmic profile as:

$$V_T(z) = V_T(z_0) \frac{\ln(z/z_R)}{\ln(z_0/z_R)} \qquad (9)$$

where $z_0 = 10$ m is the classical reference height and z_R a roughness length that depends of the sea state. However at the

scale of a sailboat mast, a linearization of this function in the vicinity of z_0 is usually sufficient and simplifies the analytic discussion. We will thus write:

$$V_T(z) = V_{10}[1 + G(z - z_0)] \qquad (10)$$

with $V_{10} = V_T(z_0)$. The usual values of the wind gradient G are of the order of 1%/m.

Note that Earth's rotation (Coriolis force) also induces a vertical evolution of the direction of the true wind, a phenomenon known as the Ekman spiral [14]. However this effect is only significant at a larger altitude of the order of 1000 m, and can therefore be safely neglected at the scale of a sailboat's mast.

Let's write down the consequence for the AWA of a vertical gradient of the true wind. The derivation of Eq. 4 with respect to z gives:

$$\frac{d\beta}{dz} = \frac{\sin \gamma}{\sin^2 \gamma + (\cos \gamma + X_{10})^2} X_{10} G. \qquad (11)$$

The evolution of AWA is then written at the same linear order

$$\beta(z) = \beta_{10} + \frac{d\beta}{dz}(z - z_0). \qquad (12)$$

This equation shows that the AWA increases linearly with altitude. The twist of the apparent wind remains proportional to the true wind gradient, but the proportionality factor is a function of the speed ratio calculated at 10 meters X_{10} and of the TWA γ. Equation 11 shows that, when the speed ratio is small, the twist is proportional to this speed ratio (with a very small effect on a slow sailboat) but that the twist decreases again for the highest speed ratios. Figure 6 shows this twist as a function of heading, and shows that the twist is maximum when running downwind. Figure 7 shows the twist of the AWA as a function of heading for different speed ratios. This figure shows that the twist of the AWA is maximum when the boat sails at the true wind velocity ($X = 1$). Note that the twist is not a unique function of the apparent wind angle β_{10} because, even at constant β_{10}, its remains dependent of X or γ.

Not that, even at high speed ratios, a residual twist of the sail may be necessary, not because the wind angles change considerably with altitude, but to limit the heeling or to decrease the induced drag. Indeed, for an un-twisted wing or sail, the optimal shape to minimize induced drag for a non twisted surface is an ellipse [2, 4]. However, the current trend is rather to install square-topped mainsails for which a twist of the sail is desirable to achieve this "elliptic load" and minimize the induced drag. In conclusion the optimal twist of the sails may be larger than the apparent wind twist (Equ. 12) for two main
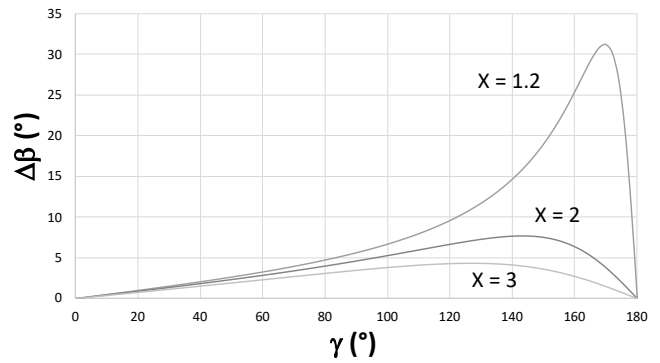

Figure 6: Twist of the apparent wind angle $\Delta\beta$ as a function of γ for a 20 m height mast in a wind gradient $G = 1$ %/m and for three values of X: 1.2, 2 and 3.
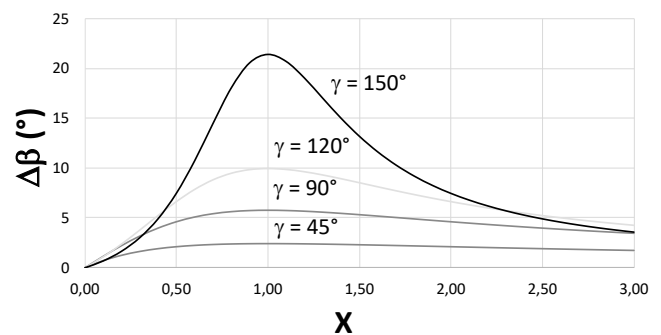

Figure 7: Twist of the apparent wind angle $\Delta\beta$ as a function of X for 20 m height mast in a wind gradient $G = 1$ %/m and for 4 values of γ: 45°, 90°, 120° and 150°.

reasons: (i) to adjust the distribution of lift along the height in order to minimize the induced drag, and (ii) to unload the top of the sails in order to lower the center of effort and reduce the heeling moment.

5 CONCLUSIONS

Some consequences of high-speed navigation were presented. For yachts using hydrofoils, we showed that a hysteresis cycle could be observed for increasing and decreasing wind conditions, depending on whether the hull is completely above water or not. This transition, which can also be observed when initiating full planing or surfing in waves after pumping on small skiffs, suggests new strategies to ease the transition to higher speeds. At high speeds, AWA is greatly reduced, affecting sail efficiency and the shape of the speed diagram. The possibility of sailing in different directions without having to ease or trim the sails was presented, and finally the effect of wind strengthening with altitude was discussed as it influences the optimal twisting of the sails.

ACKNOWLEDGEMENTS

REFERENCES

[1] I. H. Abbott and A. E. Von Doenhoff. *Theory of wing sections: including a summary of airfoil data*. Courier Corporation, 2012.

[2] G. K. Batchelor. *Introduction to Fluid Dynamics*. Cambridge University Press, 2000.

[3] S. Bourn. A fundamental theory of sailing and its application to the design of a hydrofoil sail craft. 2001.

[4] M. Drela. *Flight vehicle aerodynamics*. MIT Press, 2014.

[5] R. G. J. Flay, N. J. Locke, and G. D. Mallinson. Model tests of twisted flow wind tunnel designs for testing yacht sails. *Journal of wind engineering and industrial aerodynamics*, 63(1-3):155–169, 1996.

[6] F. Fossati. *Aero-hydrodynamics and the Performance of Sailing Yachts: The Science Behind Sailing Yachts and Their Design*. Adlard Coles, 2009.

[7] J. R. Garratt. The atmospheric boundary layer. *Earth-Science Reviews*, 37(1-2):89–134, 1994.

[8] R. Garrett. *Symmetry of sailing : The physics of sailing for yachtsmen*. Sheridan House edition, 1987.

[9] S. Heier. *Grid integration of wind energy: onshore and offshore conversion systems*. John Wiley & Sons, 2014.

[10] P. Kerdraon, B. Horel, P. Bot, A. Letourneur, D. Le Touze, et al. 6DOF behavior of an offshore racing trimaran in an unsteady environment. In *SNAME 23rd Chesapeake Sailing Yacht Symposium*. The Society of Naval Architects and Marine Engineers, 2019.

[11] J. Kimball. *Physics of Sailing*. CRC Press, 2010.

[12] P. K. Kundu. *Fluid Mechanics*. Academic Press, 1990.

[13] L. Larsson and R. E. Eliasson. *Principles of yacht design*. Adlard Coles Nautical, 2000.

[14] D. J. Tritton. *Physical fluid dynamics*. Oxford science publications, 1988.

AUTHOR BIOGRAPHY

M. Rabaud holds the current position of Professor of Fluid Mechanics at the Université Paris-Saclay. His previous experience includes fluid instabilities, turbulence, ship wakes and wind-waves formation (http://www.fast.u-psud.fr/~rabaud/).